



HAL
open science

Lithium isotopes in the Loire River Basin (France): hydrogeochemical characterizations at two complementary scales

Romain Millot, Philippe Négrel

► **To cite this version:**

Romain Millot, Philippe Négrel. Lithium isotopes in the Loire River Basin (France): hydrogeochemical characterizations at two complementary scales. *Applied Geochemistry*, 2021, 125 (104831), 10.1016/j.apgeochem.2020.104831 . hal-03113284

HAL Id: hal-03113284

<https://brgm.hal.science/hal-03113284>

Submitted on 18 Jan 2021

HAL is a multi-disciplinary open access archive for the deposit and dissemination of scientific research documents, whether they are published or not. The documents may come from teaching and research institutions in France or abroad, or from public or private research centers.

L'archive ouverte pluridisciplinaire **HAL**, est destinée au dépôt et à la diffusion de documents scientifiques de niveau recherche, publiés ou non, émanant des établissements d'enseignement et de recherche français ou étrangers, des laboratoires publics ou privés.

Lithium isotopes in the Loire River Basin (France):

hydrogeochemical characterizations at two complementary scales

Romain Millot and Philippe Négrel

BRGM, F-45060 Orléans, France

* Corresponding author : r.millot@brgm.fr

Abstract

We illustrate two different, but complementary, applications of lithium (Li) isotope tracers for river-basin characterization at two different scales within the Loire River basin (LRB) in France. The first example deals with the behaviour of Li and the fractionation of its isotopes during river weathering at the basin scale of the LRB (117,800 km²). The wide $\delta^7\text{Li}$ range (+5.0 to +13.3‰) in Loire basin streams, spatialized between the headwaters and the lowlands, is consistent with distinct weathering conditions and the distribution of Li from bedrock in the basin between the rivers and secondary mineral phases during water/rock interaction. Additionally, suspended sediments in the LRB streams are significantly ⁶Li enriched ($\delta^7\text{Li}$ from -8.7 to -7.6‰) compared to average river waters that range from +5.0 to +13.3‰. The second example focuses on the smaller scale Egoutier watershed (13 km²), part of the LRB, which shows that Li isotopes can be useful for distinguishing between natural input and anthropogenic pollution, like effluents from a water treatment plant connected to a hospital. Overall, we confirm that Li isotopes cannot be used as lithological tracers for river waters. However, we did find that Li isotopes can be good tracers of weathering conditions and of anthropogenic sources in an urbanized watershed.

Keywords: lithium isotopes, river water, sediment, Loire River Basin, wastewater, anthropogenic input, natural spring

4872 words (without references or captions)

1- INTRODUCTION

27

28 In the Earth Sciences, the field of stable-isotope geochemistry of metals has greatly expanded over
29 the past 20 years ([Johnson et al., 2004](#); [Teng et al., 2017](#)), which is mainly due to the recent
30 introduction of a new generation of Multi Collector Inductively Coupled Plasma Mass Spectrometers
31 (MC-ICP-MS) with enhanced sensitivity and better precision. These instrumental innovations have
32 opened new fields of research in metal-isotopes geochemistry ([Albarède et al., 2004](#); [Wiederhold,](#)
33 [2015](#)).

34 Among the stable-isotope systematics of metals studied so far, the geochemistry of lithium
35 (Li) has an excellent potential as a tracer of water/rock interactions within low- and high-
36 temperature systems ([Tomascak 2004](#); [Burton and Vigier 2011](#); [Tomascak et al., 2016](#); [Penniston-](#)
37 [Dorland et al., 2017](#)), whether in the field of surface waters ([Huh et al., 1998](#); [2001](#); [Vigier et al.,](#)
38 [2009](#); [Wimpenny et al., 2010](#); [Millot et al., 2010a](#); [Dellinger et al., 2014](#); [2015](#)), groundwaters ([Hogan](#)
39 [and Blum 2003](#); [Négrelet et al., 2010](#); [2012](#); [Meredith et al., 2013](#); [Pogge von Strandmann et al., 2014](#);
40 [Bagard et al., 2015](#)), geothermal waters ([Millot and Négrelet, 2007](#); [Millot et al., 2007](#); [Millot et al.,](#)
41 [2010b](#); [Millot et al., 2011](#); [2012](#); [Bernal et al., 2014](#)), rainwaters ([Millot et al., 2010c](#)) or Li-rich brines
42 ([Godfrey et al., 2013](#); [Araoka et al., 2014](#)).

43 Li isotopes are good tracers in geochemistry due to their involvement in water/rock
44 interactions at the Earth's surface. More precisely, Li and its isotopes can provide key information on
45 continental silicate weathering, which is the primary natural drawdown process of atmospheric CO₂
46 and a major control on climate ([Pogge von Strandmann et al., 2020](#)). Li isotopes help our
47 understanding of weathering via globally important processes, such as clay formation and cation
48 retention. Both these processes occur as part of weathering in surface environments, including
49 rivers, soil pore waters, and groundwater, but Li isotopes can also be used for tracking weathering
50 changes across major climate-change events ([Misra and Froelich, 2012](#)).

51 Furthermore, Li has a strategic importance for numerous industrial applications, including the
52 production of Li-ion batteries for mobile devices and electric vehicles ([World Economic Forum](#)

53 [Report, 2019](#)), or in pharmaceuticals used in the treatment of some mental diseases ([Aral and](#)
54 [Vecchio-Sadus 2008; 2011](#)).

55 Assessing the behaviour of Li and its isotopes during chemical weathering is important for a
56 better definition of water/rock interactions at the Earth's surface and also for refining our
57 understanding of the global Li cycle. Lithium (${}^6\text{Li} \sim 7.5\%$ and ${}^7\text{Li} \sim 92.5\%$) is a fluid, mobile metallic
58 element and, due to the large relative mass difference between its two stable isotopes, it is subject
59 to significant low-temperature mass fractionation that provides key information on weathering
60 processes.

61 Additionally, the contribution of human activities (industry, agriculture, and domestic inputs)
62 becomes increasingly significant in the chemical composition of dissolved river load ([Aral and](#)
63 [Vecchio-Sadus 2008; 2011](#)) as well as in that of soil ([Négrel et al., 2019](#)). Human factors thus act as an
64 additional key process and, therefore, a mass-balance for the budget of catchments and river basins
65 must also consider anthropogenic disturbance of Li ([Choi et al., 2019](#); [Négrel et al., 2020](#)).

66 To date, both the magnitude of Li-isotopic fractionation associated with water/rock
67 interaction processes, and the factors controlling such fractionation, are not totally understood.
68 However, both field- and experimental studies have shown that ${}^6\text{Li}$ is preferentially retained by
69 secondary minerals during silicate weathering ([Pistiner and Henderson 2003](#), [Kisakürek et al. 2004](#),
70 [Pogge von Strandmann et al. 2006](#), [Vigier et al. 2009](#)). Accordingly, the fractionation of Li isotopes
71 depends upon the extent of chemical weathering: strong fractionation seems to occur during
72 incipient and early weathering stages, while little fractionation is observed during more intense or
73 prolonged weathering in a stable environment, such as a low plain with long residence times; [Huh et](#)
74 [al. 1998, 2001](#), [Pogge von Strandmann et al. 2006](#), [Millot et al., 2010a](#)).

75 Li-isotope fractionation has been documented in numerous natural environments with
76 experimental and natural data ([Tomascak 2004](#), [Burton and Vigier 2011](#); [Tomascak et al., 2016](#);
77 [Penniston-Dorland et al., 2017](#); [Pogge von Strandmann et al., 2020](#)). It was shown that partial
78 dissolution of basalt does not result in Li-isotope fractionation, but that granite dissolution can cause

79 such fractionation ([Pistiner and Henderson 2003](#); [Négre and Millot, 2019](#)). In addition, adsorption
80 onto mineral surfaces can be another major mechanism of Li-isotopic fractionation in the
81 hydrosphere ([Wenshuai and Liu, 2020](#); [Andrews et al., 2020](#)). Moreover, Li is not a nutrient and does
82 not participate in biologically mediated reactions, so no evidence of biological Li-isotope
83 fractionation has been observed to date ([Rudnick et al., 2004](#); [Marriott et al., 2004](#)).

84 Here, we illustrate two applications at complementary scales of Li isotopes used for river-
85 basin hydrogeochemical surveys. The first example deals with the behaviour of Li and its isotopes at
86 the Loire basin (LRB) scale (117,800 km², France) for river water and sediment transported during
87 river flow. The second example focuses on a smaller scale: the Egoutier watershed (13 km²), part of
88 the LRB. The main objective of our work was to evaluate Li isotopes as 1) tracers of weathering
89 conditions over a large river basin, and 2) tracers of anthropogenic input at the scale of a small
90 watershed.

91 2- ANALYTICAL METHODS

92 2.1. Sampling methods and element concentration measurements

93 In the LRB ([Table 1](#)), river waters were sampled twice, first during low flow and then during high flow
94 (August/September 2012 and April 2013, respectively). Suspended sediments in the Loire at
95 Montjean (the farthest downstream sampling station of this study, 955 km from the Loire spring)
96 were sampled monthly between July 2012 and June 2013. For the Egoutier watershed, we collected
97 river water in April 2015), corresponding to the high-flow stage of the watershed.

98 In the field, 5 litres of river water were collected in acid-washed containers for major- and
99 trace-element and isotopic measurements (for details of the protocol see [Millot et al., 2003](#)).
100 Samples were filtered in the field, using a Sartorius frontal filtration unit (0.2 µm cellulose acetate
101 filter, 142 mm diameter). After filtration, samples were stored in acid-washed polypropylene bottles.
102 The river sediments were collected after drying and centrifugation of the river-water filtration
103 retentate. The samples for Li-concentration and Li-isotope analyses were acidified to pH=2 with
104 ultrapure HNO₃. Lithium concentrations in river-water and suspended-sediment samples were

105 determined by Quadrupole ICP-MS (Thermo X Series II) with indium as an internal standard, with a
106 precision of $\pm 5\%$.

107 **2.2 Lithium isotope measurements**

108 Lithium-isotopic compositions were measured using a Neptune⁺ Multi-Collector ICP-MS at the BRGM
109 (French Geological Survey; [Millot et al., 2004](#)). $^7\text{Li}/^6\text{Li}$ ratios were normalized to the L-SVEC standard
110 solution (NIST SRM 8545, [Flesch et al., 1973](#)) following the standard-sample bracketing method.
111 Typical in-run precision on the determination of $\delta^7\text{Li}$ was about 0.1-0.2‰ ($2\sigma_m$, standard error of the
112 mean). Chemical separation of Li from the matrix before isotope analyses was done with a cationic
113 exchange resin (a single column filled with 3 mL of BioRad AG[®] 50W-X12 resin, 200-400 mesh) and
114 HCl acid (0.2N) rendering 30 ng Li. Blanks for the total chemical extraction were <30 pg Li, which is
115 negligible as this represents a blank/sample ratio of $<10^{-3}$.

116 Successful quantitative measurement of Li-isotopic compositions requires 100% Li recovery
117 during laboratory processing. Therefore, frequent column calibrations were performed and repeated
118 analysis of an L-SVEC standard processed through the columns showed that no isotope fractionation
119 occurred as a result of the purification process.

120 The accuracy and reproducibility of the entire method (purification procedure + mass
121 analysis) were also tested by repeated measurement of a seawater standard solution (IRMM BCR-
122 403) after separation of Li from the matrix, giving a mean value of $\delta^7\text{Li} +30.8 \pm 0.4\%$ (2σ , $n=15$) over
123 the duration of the analyses. This mean value agrees with our long-term measurements ($\delta^7\text{Li} +31.0$
124 $\pm 0.5\%$, 2σ , $n=30$, [Millot et al., 2004](#)) and with other values reported in the literature (see for
125 example [Carignan et al., 2004](#) and [Tomascak 2004](#) for a data compilation).

126 For suspended sediments, a total digestion of 50 mg of crushed sample took place over
127 4 days at 100 °C in a closed beaker with a mixture of three ultrapure acids: 4 mL HF (23N), 1 mL HNO₃
128 (14N) and 0.1 mL HClO₄ (12N). The solution obtained was evaporated to dryness and 4 mL HCl (6N)
129 was added and left for a further 4 days at 100 °C. Sample aliquots (30 ng Li) of the residue of the acid
130 dissolution were then dissolved in 0.5 mL HCl (0.2N), before being placed in cation exchange columns

131 for Li separation. Accuracy and reproducibility of the entire procedure for solid samples (dissolution +
132 purification + mass analysis) were tested by repeated measurements of the JB-2 basalt standard
133 (Geological Survey of Japan), which gave a mean value of $\delta^7\text{Li} = +4.9\text{‰} \pm 0.6\text{‰}$ (2σ , $n=17$), in good
134 agreement with published values (see [Jeffcoate et al. 2004](#), [Tomascak 2004](#) and [Carignan et al. 2007](#)
135 for data compilation).

136 3- FIELD SITE DESCRIPTION

137 3.1 The Loire River Basin

138 We undertook a systematic study of the weathering products (both dissolved load and suspended
139 sediments) of the LRB, one of the major river basins in Europe. This area is of particular interest as it
140 has been extensively studied and is scientifically well characterized ([Négrel and Grosbois 1999](#);
141 [Grosbois et al., 2001](#)).

142 The Loire River in central France ([Fig. 1](#)) is approximately 1010 km long and drains an area of
143 117,800 km². Initially, the Loire flows north to northwest, originating in the Massif Central and
144 continuing up to the city of Orléans, about 650 km from the source. Beyond Orléans, the river turns
145 west to WSW, being one of the main European riverine inputs into the Atlantic Ocean. In the upper
146 basin, the bedrock is Palaeozoic plutonic rock overlain by sub-Recent volcanic rocks. The
147 intermediate basin includes three major tributaries flowing into the Loire from the left bank: the
148 Cher, the Indre and the Vienne rivers. Here, the Loire drains sedimentary rocks of the Paris Basin,
149 mainly carbonate deposits. The lower Loire basin drains Palaeozoic basement rocks of the Armorican
150 Massif and its overlying Mesozoic to Cenozoic sedimentary deposits.

151 Its spring is located at an altitude of 1,404 m (Mont Gerbier de Jonc) and its course is
152 classically divided into three parts from upstream to downstream: (i) the Upper Loire, (ii) the Loire
153 Valley, and (iii) the Lower-Loire, to the estuary. River discharge of the Loire is very irregular: in the
154 Lower Loire it can exceed 7000 m³/s, but at Orléans it is around 350 m³/s and during summer the
155 river can literally dry up, with flows less than 25 m³/s.

156 BRGM's expert knowledge of the LRB is recognized by the numerous, particularly isotopic,
157 studies, that have been carried out over the past decades (Négre, 1997; Négre and Grosbois, 1999;
158 Négre et al., 2000; Négre and Petelet-Giraud, 2012; Petelet-Giraud et al., 2018). The Loire has been
159 regularly monitored at Orléans and Tours over several hydrological cycles (Grosbois et al., 2000;
160 2001). Its physico-chemical parameters, major- and trace elements, and strontium-isotope ratios
161 were determined on the dissolved fraction over time spans ranging from two days to one week,
162 depending on river flow.

163 The relationships between chemical elements and flow as well as between isotopic ratios and
164 flow have shown that the dissolved fraction of the Loire results from a mixture between rainfall
165 input, input from the weathering of silicate- and carbonate bedrocks, and anthropogenic input of
166 agricultural and urban origin. Total dissolved-solids flow during a hydrological cycle is estimated at
167 1300×10^3 t/year at Orléans and 1620×10^3 t/year at Tours (Grosbois et al., 2001). For the river
168 sediments, work by Négre and Grosbois (1999) on $^{87}\text{Sr}/^{86}\text{Sr}$ isotope ratios suggests the existence of
169 at least two reservoirs of suspended matter transported by the river. One is related to the detrital
170 fraction from silicate erosion, the other to carbonate erosion. The stable isotopes of carbon and
171 oxygen in the fraction extracted by acid leaching from Loire sediments during periods of low water
172 flow (Négre et al., 2000), confirm the formation of antigenic calcites in isotopic equilibrium with
173 Loire water (Fontes et al., 1973; Dever et al., 1983).

174 **3.2 The Egoutier watershed**

175 We also investigated anthropogenic Li tracing of wastewater release, using Li isotopes in the small
176 Egoutier catchment near Orléans (13 km², Fig. 2; in French, 'Egout' means 'Sewer', Desaulty and
177 Millot 2017).

178 Located in the Paris Basin on the Beauce plateau just east of Orléans, the Egoutier is a small
179 stream with its spring near the village of Chanteau and a length of 5 km before being channelled and
180 flowing into the Loire at Saint-Jean-de-Braye. For this study, we worked in a small built-up area

181 between its spring in the forest and a point just downstream of the departmental road D2060
182 (Fig. 2).

183 The study area integrates two main potential sources of metals due to human activities: The
184 first one is a psychiatric hospital with about 300 beds and many outpatients. The hospital also houses
185 an active laundry. About a ton of linen from different community sources (fire brigade, schools, etc.)
186 is washed and ironed every day. The second one is an industrial area including a slaughterhouse,
187 factories for processing animal products, and the oil depot of Saint-Jean-de-Braye that supplies fuel
188 oil to the Centre-Val-de-Loire region. This second area is drained by a stream that flows into the
189 Egoutier.

190 4- RESULTS

191 4.1 The Loire River basin

192 In the LRB (Table 1), natural Li concentrations in river water are between 2.0 and 46.5 µg/L whereas
193 $\delta^7\text{Li}$ -isotopic compositions range from +5.0 to +13.3‰. In more detail, there are slight differences
194 depending upon whether the rivers were sampled during low- or high-flow stages.

195 During low flow, Li concentrations are higher (3.4 to 46.5 µg/L; mean 15.9 µg/L n=20, Table 1) than
196 during high flow (Li concentrations from 2.0 to 30.0 µg/L with a mean of 7.4 µg/L, n=20, Table 1). In
197 parallel, the Li-isotopic compositions are little different for low- and high-flow samples, with $\delta^7\text{Li}$
198 values ranging from +5.0 to +13.3‰ and +5.2 to +11.7‰ respectively. These concentrations are
199 higher than the worldwide riverine average of 1.9 µg/L (Huh et al., 1998; Gaillardet et al., 2014). In
200 addition, Loire basin rivers have lower isotopic compositions than the average $\delta^7\text{Li}$ value for modern
201 river water of about +23‰ (Huh et al., 1998; Misra and Froelich, 2012). Finally, $\delta^7\text{Li}$ values for the
202 Loire basin rivers agree with previous data reported by Rivé et al. (2013) for the upstream Loire ($\delta^7\text{Li}$
203 from 4.0 to 24.0‰). Loire river suspended sediments collected monthly at Montjean/Loire (Table 2)
204 from July 2012 to June 2013 have Li concentrations between 41.3 and 73.0 µg/g (mean 60.2 µg/g,
205 n=7), significantly higher than those of the average Upper Continental Crust (UCC) at Li 35 ± 11 µg/g
206 (2σ , Teng et al., 2004). In addition, these sediments have low $\delta^7\text{Li}$ with strongly negative values

207 ranging from -8.7 to -7.6‰ (mean 8.2‰, n=7) when compared to the UCC value of 0‰ ±2 (Teng et
208 al., 2004).

209 **4.2 The Egoutier watershed**

210 Lithium concentrations in the Egoutier watershed cover a narrow range from 5.3 to 12.7 µg/L (mean
211 7.3 µg/L, n=9, Table 3), whereas the isotopic compositions of Li are comprised between -3.1 and
212 +4.2‰ (mean +0.5‰, n=10, Table 3). The Li concentrations and the $\delta^7\text{Li}$ values in the Egoutier
213 watershed are very different from the ones observed at the larger scale of the LRB.

214 **5- DISCUSSION**

215 **5.1 The Loire River basin: controlling parameters for the distribution of Li and its isotopes**

216 Overall, Li concentrations in Loire River mainstream waters span a wide range from 2.0 to 22.5 µg/L,
217 whereas $\delta^7\text{Li}$ values are between +5.9 and +13.2‰ (Table 1). Figures 3a and 3b show a clear contrast
218 for the main course of the Loire River between headwaters and lowlands. This contrast shows a
219 significant increase in Li concentrations from upstream to downstream (Fig. 3a). This feature is also
220 associated with a strong decrease in the $\delta^7\text{Li}$ values as a function of distance from the spring. These
221 variations for Li concentration and $\delta^7\text{Li}$ are observed for both high and low flow stages.

222 In addition, when all $\delta^7\text{Li}$ values are plotted for both the Loire and its major tributaries (Cher,
223 Indre, Vienne, Maine, Furan, Arroux and Allier rivers, Fig. 1) in a $\delta^7\text{Li}$ vs. Na/Li diagram (Fig. 4), the
224 data plot in a triangle formed by three endmembers. The first (Na/Li ~8000 and $\delta^7\text{Li}$ ~+12‰) is the
225 upstream Loire at Villerest; the second endmember is close to the Allier river (Na/Li ~500 and $\delta^7\text{Li}$
226 ~+5‰); and the third could be represented by rainwater. This agrees with the conceptual scheme of
227 the Loire hydrosystem based on $\delta^{18}\text{O}$ and $^{87}\text{Sr}/^{86}\text{Sr}$ data, suggesting that the Loire River is related to a
228 Massif Central surface-water supply for the main Loire and Allier streams, and to water/groundwater
229 interactions in the alluvial plains (Négrel et al., 2003).

230 For the second endmember, the Allier constitutes a major tributary of the Loire that mostly
231 drains the French Massif Central. As a result, its chemical (Na/Li) and isotopic signatures are
232 influenced by input from thermo-mineralized waters resulting from hydrothermal activity, as

233 demonstrated by [Négrel et al. \(1997\)](#). These thermal springs are well described for the whole Massif
234 Central area and have low $\delta^7\text{Li}$ values ([Fig. 4](#), [Millot et al., 2007](#)). The third endmember,
235 corresponding to rainwater input, is in a good agreement with our long-term monitoring values of
236 rainwater at Orléans and also near Clermont-Ferrand within the Massif Central, corresponding to the
237 continental signature of rainwaters in France ([Millot et al., 2010c](#)).

238 It is well known that rainfall on watersheds can supply an important fraction of dissolved
239 elements in river water ([Meybeck, 1983](#)). Atmospheric correction requires knowledge of the
240 chemical composition of rainwater (*op. cit.*; [Négrel et al., 1993](#)). The correction of atmospheric
241 contribution to water, for a given element Z, is estimated by reference to the Cl concentration, called
242 Cl_{ref} , multiplied by the Z/Cl ratio of rainwater. For the LRB and according to [Grosbois et al. \(2000\)](#), we
243 considered the Cl_{ref} at 2.62 $\mu\text{g/L}$ (74 $\mu\text{mol/L}$). We applied the atmospheric correction to Na, Li and
244 $\delta^7\text{Li}$ values, as earlier done for other studies on Li isotopes ([Dellinger et al., 2015](#); [Négrel and Millot,](#)
245 [2019](#); [Négrel et al., 2020](#)). Here, we used the characterization of rainwater defined by [Négrel and Roy](#)
246 [\(1998\)](#), [Négrel et al. \(2007\)](#) and [Millot et al. \(2010c\)](#), who reported major ions, but also Li
247 concentrations and isotopes ([Millot et al., 2010c](#)). The different rainfall stations in France range from
248 near-ocean locations (Brest, Dax) to more continental ones (Orléans). The latter has the lowest Li
249 concentrations (0.37 $\mu\text{g/L}$) and $\delta^7\text{Li}$ values (+16.1‰). In view of its continental character, this station
250 is certainly the one that can best match the rain input over the LRB. [Table 1](#) shows that Li in waters
251 from atmospheric origin ranges from 1.2 to 16.8% and from 1.9 to 28.2%, respectively for low- and
252 high-flow stages.

253 Once atmospheric correction was applied to lithium and its isotopes ([Table 1](#); [Fig. 5](#)), the Li-
254 isotopic compositions of the Loire River were spatialized along the main course. [Figure 5](#) shows $\delta^7\text{Li}$
255 values plotted against Li concentrations: we see two parallel lines, one for high flow stages and the
256 second for low flow ones. The two lines are not interpreted as a mixing scheme for which the trends
257 may not be linear in such a representation. Nor could this feature be interpreted as a result of a
258 lithological contrast between the upstream and downstream Loire River (plutonic/volcanic rocks vs.

259 sedimentary deposits), in agreement with the results of [Kısakürek et al. \(2005\)](#), [Vigier et al \(2009\)](#) and
260 [Millot et al. \(2010a\)](#) that showed that Li isotopes cannot be used as lithological tracers in river basins.

261 This general picture might thus be better explained in terms of water/rock interaction: in the
262 upstream environments of the Loire basin, short water-residence times and rock weathering may
263 enhance processes that fractionate Li isotopes, such as adsorption and/or secondary-mineral-phase
264 formation, producing high $\delta^7\text{Li}$ in rivers ([Négreil and Millot, 2019](#)). By contrast, in the lowlands of the
265 Loire basin, longer water-residence time could enhance Li dissolution, with lower isotopic
266 fractionation (low $\delta^7\text{Li}$) approaching that of continental bedrock. Such a Li-isotope distribution has
267 already been reported for other large river basins, worldwide ([Lemarchand et al., 2010](#); [Millot et al.,](#)
268 [2010b](#); [Liu et al., 2013](#); [2015](#); [Dellinger et al., 2014](#); [2015](#); [Wang et al., 2015](#)).

269 More specifically, the Li-isotopic composition measured in the Loire basin rivers shows that
270 the dissolved load is significantly enriched in ^7Li when compared to suspended river load. Lithium
271 concentrations in suspended Loire sediment at Montjean ([Table 2](#)) contain 41 to 73 $\mu\text{g/g}$ and are
272 clearly ^6Li enriched; $\delta^7\text{Li}$ values being negative (-8.7 to -7.6‰), compared to dissolved loads (+5.0 and
273 +13.0‰). This result agrees with the fact that ^6Li is preferentially incorporated into suspended
274 sediment during weathering as also observed for other river basins worldwide ([Huh et al. 1998, 2001,](#)
275 [Pogge von Strandmann et al. 2006, Millot et al., 2010b](#)).

276 Finally, the relationship between $\delta^7\text{Li}$ and Al/Li in the suspended sediment ([Fig. 6](#)) could also
277 raise the question of the control by different mineral phases (clay minerals vs. oxy-hydroxide of Fe or
278 Mn, or carbonates) during Li-isotopic fractionation between water and solids. The variation of the
279 Al/Li ratio could reflect a compositional variation of clay minerals in suspended sediments. It is also
280 likely that the suspended sediments consist of both fine (clay rich) and coarse (carbonate rich)
281 factions.

282 Unfortunately, we do not dispose over specific mineral-characterization data on our samples
283 for further discussion of this point, but it is interesting to observe an inverse correlation between the
284 Li-isotope signatures of suspended sediments and the river discharge ([Fig. 7](#)). This trend could

285 possibly suggest at least two different sources for suspended sediments, one during high flow and
286 the other during low flow, agreeing with the results from Sr-isotopic ratios of the Loire sediments
287 (Négrel et al., 2000; Négrel and Roy, 2002).

288 A final point that might explain such a relationship could be that the $\delta^7\text{Li}$ content in solids
289 may reflect weathering intensity (i.e., soil formation/transformation, coarse/fine material), as argued
290 by Dellinger et al. (2014; 2015). Consequently, different pools of river sediments are likely to be
291 transported as a function of the river regime.

292 **5.2 Anthropogenic origin of Li in the Egoutier watershed**

293 Human activities such as industry, agriculture and domestic inputs, generally increase the quantity
294 and modify the quality of chemical compounds in the dissolved and suspended load of rivers (Viers et
295 al., 2009; Royer, 2016; Vanwallegem et al., 2017). Human factors can also act as another key
296 process for Li in rivers (Choi et al., 2019; Négrel et al., 2020). Therefore, the mass-balance for the
297 budget of catchments and river basins should include anthropogenic disturbance.

298 Here, we investigate the effect of wastewater release by tracing its impact through using Li
299 isotopes in the small Egoutier watershed (13 km², 5 km long). As a case study, we studied this small
300 watershed with a low housing density in the LRB (Ledieu et al., 2020). Its spring is located in a pristine
301 forested area, but some kilometres downstream it is affected by metal-rich effluents from a hospital
302 water-treatment plant as well as by input from an industrial area (Fig. 2, Desaulty and Millot, 2017).

303 Within the course of the Egoutier, we clearly see the impact of both human activities. When
304 Li concentrations are plotted as a function of distance from the spring (Fig. 8a), we see two different
305 inputs: one from the waste water treatment plant (WWTP) related to the psychiatric hospital and the
306 second from the stream draining the industrial area.

307 Whereas the natural background for Li in river waters is 5 to 6 $\mu\text{g/L}$, the values for the
308 Hospital WWTP release and the industrial area are 12.7 $\mu\text{g/L}$ and 9.4 $\mu\text{g/L}$, respectively. In addition,
309 Li-isotopic compositions are rather homogeneous in water of the Egoutier watershed, with $\delta^7\text{Li}$
310 values of around $+0.5\% \pm 1.2$ along the main course of the stream ($n=7$, grey arrow on Fig. 8b), but

311 the signatures of the hospital and industrial area releases are very different. The WWTP water has a
312 positive $\delta^7\text{Li}$ value of +4.2‰, whereas the stream draining the industrial area has a negative value at -
313 3.1‰. The two anthropogenic signatures are quite different for Li isotopes. As mentioned before, the
314 hospital is a psychiatric one and it is likely that the Li released by the WWTP mainly comes from
315 pharmaceutical products, such as Li carbonate used for bipolar disease treatment ([Machado-Vieira et](#)
316 [al., 2009](#)). The nearby industrial area is mostly impacted by effluents from a slaughterhouse and
317 animal-processing operations ([Desauty and Millot, 2017](#)).

318 These observations in the Egoutier watershed completely agree with recent work by [Choi et](#)
319 [al. \(2019\)](#), who investigated the impact of anthropogenic input on lithium content in river- and tap
320 waters within the metropolitan area of Seoul, South Korea. They showed that Li-enriched
321 wastewater can affect tap waters. They also report Li-isotopic signatures of both therapeutic drugs
322 (Li carbonate) and detergents that are compatible with our findings for the wastewater treatment
323 plant releases in the Egoutier, which combine waste from the laundry and the psychiatric hospital.

324 This example of the Egoutier watershed shows how Li isotopes can distinguish between
325 natural and anthropic origins at the scale of a small watershed. This ability was recently evoked for
326 Seoul (South Korea; [Choi et al. 2019](#)) as well as for the Dommel catchment (Belgium and
327 Netherlands; [Négrel et al., 2020](#)). In both cases, lithium and its isotopes are effective tracers of
328 wastewater releases in populated areas, as well as of industrial discharge (smelter effluents) into a
329 river, respectively.

330 Further investigations are now needed to more precisely determine the Li-isotopic
331 compositions of pharmaceutical formulations, but also the role of wastewater treatment processes
332 in the distribution of metals between liquid and solid phases within a treatment plant. The latter
333 point is particularly relevant, as [Choi and al. \(2019\)](#) showed that there is no significant difference
334 between influent and effluent waters for both Li concentrations and Li isotope compositions, thus
335 making this tracer a perfect conservative tool for tracing Li pollution in the environment.

336 This study can be considered as pioneering, since Li is found naturally in drinking water (Eyre-
337 Watt et al., 2020; Ewuzie et al., 2020) with various origins. In clinical practice, it is widely used in the
338 treatment of bipolar and of mood disorders. And, very importantly because of the increasing
339 production of lithium-ion batteries worldwide (Naish et al., 2008; Conolly 2010; Christmann et al.,
340 2015), Li pollution in surface- and groundwaters could become a major issue in coming years, as
341 recently suggested by Choi et al. (2019).

342 6- CONCLUDING REMARKS AND FUTURE DIRECTIONS

343 A large variability of Li-isotopic ratios exists within the Loire river basin (LRB) and $\delta^7\text{Li}$ is strongly
344 spatialized between the Loire headwaters and lowlands. In addition, the Allier river, a major tributary
345 in the French Massif Central, is clearly influenced by the contribution of thermo-mineral springs with
346 lower $\delta^7\text{Li}$. Suspended river sediments are ^6Li enriched ($\delta^7\text{Li}$ from -8.7 to -7.6‰) compared to river
347 waters (+5.0 to +13.3‰), agreeing with the fact that ^6Li is preferentially incorporated in suspended
348 sediments.

349 Overall, although the weathering mechanisms operating in the LRB must be defined in much
350 more detail, our work confirms that Li isotopes cannot be used as lithological tracers for river waters.
351 However, we also show that Li isotopes are good tracers of river weathering conditions, with an
352 innovative application for tracing anthropogenic Li sources in a small, urbanized watershed. Further
353 work is now required for better characterizing the chemical and isotopic signals of pharmaceutical
354 formulations containing Li as well as those of Li-ion batteries. More specifically, leaks from landfills
355 containing electronic products must be investigated for determining whether curative work is
356 needed to stop the spread of pollutants. To conclude, lithium and $\delta^7\text{Li}$ are good proxies for studying
357 weathering and anthropogenic activities.

358

359 **Acknowledgements:**

360 This work was supported by the Research Program ISOP2 (Origin and mobility of metals in water and
361 sediment of the Loire River Basin), cofounded by BRGM and the AELB Water Agency (Agence de l'Eau

362 Loire Bretagne). Special thanks are due to S. Perret for his help in sample preparation in the clean
363 laboratory and in the field. We acknowledge our fruitful discussions with A.M. Desaulty, X. Bourrain
364 and E. Petelet-Giraud. The BRGM Water, Environment, Process Development and Analysis Division is
365 acknowledged for funding. This study was part of the Service National d'Observation Environnements
366 Urbains: OBSERVIL (French Urban Observatory), accredited by the INSU/CNRS and on site certified by
367 the Zone Atelier Loire: OBSCURE [OBServatoire des Sédiments et de la Cascade sédimentaire en
368 milieu URbain : cas de l'Egoutier à Semoy (Loiret)] managed by A. Simonneau. We thank three
369 anonymous reviewers and the Associate Editor for their constructive comments and remarks.
370 H.M. Kluijver edited the final English version of the MS for language and content.
371 RM is particularly grateful to T.D. (Tom) Bullen for helping him in the first stages of Li-isotope
372 investigations at BRGM, more than 17 years ago; this work is dedicated to his memory.
373
374

375 **References**

- 376 Albarède F., Télouk P., Blichert-Toft J., Boyet M., Agraniér A., and Nelson B. (2004). Precise and
377 accurate isotopic measurements using multiple-collector ICPMS. *Geochim. Cosmochim. Acta* 68,
378 2725-2744.
- 379 Andrews E., Pogge von Strandmann A.E., Fantle M.S. (2020). Exploring the importance of authigenic
380 clay formation in the global Li cycle. *Geochim. Cosmochim. Acta*, 289, 47-68.
- 381 Aral H., Vecchio-Sadus A. (2008). Toxicity of lithium to humans and the environment, A literature
382 review. *Ecotoxicology and Environmental Safety* 70, 349-356.
- 383 Aral H., Vecchio-Sadus A. (2011). Lithium: Environmental Pollution and Health Effects. *Encyclopedia*
384 *of Environmental Health*. pp 499-508.
- 385 Araoka D., Kawahata H., Takagi T., Watanabe Y., Nishimura K., Nishio Y. (2014). Lithium and
386 strontium isotopic systematics in playas in Nevada, USA: constraints on the origin of lithium.
387 *Mineral. Deposita* 49, 371–379.
- 388 Bagard M.L., West A.J., Newman K., Basu A.R. (2015). Lithium isotope fractionation in the Ganges-
389 Brahmaputra floodplain and implications for groundwater impact on seawater isotopic
390 composition. *Earth Planet Sci. Lett.* 432, 404–414.
- 391 Bernal N.F., Gleeson S.A., Dean A.S., Liu X.M., Hoskin P. (2014). The source of halogens in geothermal
392 fluids from the Taupo Volcanic Zone, North Island, New Zealand. *Geochim. Cosmochim. Acta* 126,
393 265–283.
- 394 Burton K.W., Vigier N. (2011). Lithium isotopes as tracers in marine and terrestrial environments
395 *Handbook of environmental isotope geochemistry. Advances in Isotope Geochemistry*. Ed. Mark
396 Baskaran. 2011, vol. 1, pp. 41-60.
- 397 Carignan J., Cardinal D., Eisenhauer A., Galy A., Rehkämper M., Wombacher F., Vigier N. (2004). A
398 reflection on Mg, Ca, Cd, Li and Si isotopic measurements and related reference materials.
399 *Geostandards and Geoanalytical Research* 28, 139-148.

400 Carignan J., Vigier N., Millot R. (2007). Three secondary reference materials for Li isotopic
401 measurements: 7Li-N, 6Li-N and LiCl-N. *Geostandards and Geoanalytical Research* 31, 7-12.

402 Choi H.B., Ryu J.S., Shin W.J., Vigier N. (2019). The impact of anthropogenic inputs on lithium content
403 in river and tap water. *Nature Communications* 10:5371 | [https://doi.org/10.1038/s41467-019-](https://doi.org/10.1038/s41467-019-13376-y)
404 [13376-y](https://doi.org/10.1038/s41467-019-13376-y)

405 Conolly D. (2010). A Review of Energy Storage Technologies: for the Integration of Fluctuating
406 Renewable Energy. Aalborg Universitet. <http://vbn.aau.dk/files/>

407 Christmann P., Gloaguen E., Labbé J.F., Melleton, J., Piantone P. (2015). Global Lithium Resources and
408 Sustainability Issues. *Lithium Process Chemistry*. Elsevier, pp. 1–40.

409 Dellinger M., Gaillardet J., Bouchez J., Calmels D., Galy V., Hilton R.G., Louvat P., France-Lanord C.
410 (2014). Lithium isotopes in large rivers reveal the cannibalistic nature of modern continental
411 weathering and erosion. *Earth Planet Sci. Lett.* 401, 359–372.

412 Dellinger M., Gaillardet J., Bouchez J., Calmels D., Louvat P., Dosseto A., Gorge C., Alanoca L., Maurice
413 L. (2015). Riverine Li isotope fractionation in the Amazon River basin controlled by the weathering
414 regimes. *Geochim. Cosmochim. Acta* 164, 71–93.

415 Desaulty A.M., Millot R. (2017). *Projet ISOP2 : Origine, mobilité et répartition eaux/sédiments des*
416 *métaux (Pb, Zn, Cu) : exemple de deux sous-bassins versants (Argos et Egoutier) du bassin Loire-*
417 *Bretagne. Rapport final. BRGM/RP-66799 -FR, 127 p.*

418 Dever L., Durand R., Fontes J.C.H., Vachier P. (1983). Étude pédogénétique et isotopique des
419 néoformations de calcite dans un sol sur Craie, Caractéristiques et origine. *Geochim. Cosmochim.*
420 *Acta* 47, 2079-2090.

421 Ewuzie U., Nnorom I.C. , Eze S.O. (2020). Lithium in drinking water sources in rural and urban
422 communities in South-eastern Nigeria. *Chemosphere* 245, 125593.

423 Eyre-Watt B, Mahendran E, Suetani S, Firth J, Kisely S, Siskind D. (2020). The association between
424 lithium in drinking water and neuropsychiatric outcomes: A systematic review and meta-analysis

425 from across 2678 regions containing 113 million . Australian & New Zealand Journal of Psychiatry.
426 October 2020. doi:10.1177/0004867420963740.

427 Flesch G.D., Anderson A.R., Svec H.J. (1973). A secondary isotopic standard for $^6\text{Li}/^7\text{Li}$ determinations.
428 International Journal of Mass Spectrometry and Ion Physics 12, 265-272.

429 Fontes J.C.H., Lepvrier C., Melieres F., Pierre C. (1973). Isotopes stables dans les carbonates
430 évaporitiques du Miocène Supérieur de Méditerranée Occidentale. In: Messinian Events in the
431 Mediterranean. Koninklijke Nederlandse Akademie van Wetenschappen, Amsterdam, pp. 91–100.

432 Gaillardet J., Viers J., Dupré B., (2014). Trace Elements in River Waters. Treat. Geochem. (second ed.)
433 7, 195–235.

434 Godfrey L.V., Chan L.H., Alonso R.N., Lowenstein T.K., McDonough W.F., Houston J., Li J., Bobst A.,
435 Jordan T.E. (2013). The role of climate in the accumulation of lithium-rich brine in the Central
436 Andes. Appl. Geochem. 38, 92–102.

437 Grosbois C., Négrel Ph., Fouillac C., Grimaud D. (2000). Dissolved load of the Loire river: Chemical and
438 isotopic characterization. Chem. Geol. 170, 179-201.

439 Grosbois C., Négrel P., Grimaud D., Fouillac C. (2001) .An overview of dissolved and suspended
440 matter fluxes in the Loire River Basin: Natural and anthropogenic inputs. Aqu. Geochem. 7, 81-
441 105.

442 Hogan J.F., Blum J.D. (2003). Boron and lithium isotopes as groundwater tracers: a study at the Fresh
443 Kills Landfill, Staten Island, New York, USA. Appl. Geochem. 18, 615–627.

444 Huh Y., Chan L.C., Zhang L., Edmond J.M. (1998). Lithium and its isotopes in major world rivers:
445 implications for weathering and the oceanic budget. Geochim. Cosmochim. Acta, 62, 2039-2051.

446 Huh Y., Chan L.C., Edmond J.M. (2001). Lithium isotopes as a probe of weathering processes: Orinoco
447 River. Earth Planet Sci. Lett. 194, 189-199.

448 Jeffcoate A.B., Elliott T., Thomas A., Bouman C. (2004). Precise, small sample size determinations of
449 lithium isotopic compositions of Geological Reference Materials and modern seawater by MC-ICP-
450 MS. Geostandards and Geoanalytical Research, 28: 161-172.

451 Johnson C.M., Beard B.L., Albarède F. (2004). Geochemistry of Non-Traditional Stable Isotopes
452 Overview and General Concepts. *Reviews in Mineralogy & Geochemistry* 55, 1-24.

453 Kısakürek B., Widdowson M., James R.H. (2004). Behaviour of Li isotopes during continental
454 weathering: the Bidar laterite profile, India. *Chem. Geol.* 212, 27-44.

455 Kısakürek B., James R.H., Harris N.B.W. (2005). Li and $\delta^7\text{Li}$ in Himalayan rivers: Proxies for silicate
456 weathering? *Earth Planet. Sci. Lett.*, 237, 387-401.

457 Ledieu L., Simonneau A., Cerdan C., Négrel Ph., Laperche V., Grosbois C., Laggoun F. (2020).
458 Geochemical insights into spatial and temporal evolution of sediments at catchment scale. *Appl.*
459 *Geochem.* 104743.

460 Lemarchand E., Chabaux F., Vigier N., Millot R., Pierret M.C. (2010). Lithium isotope systematics in a
461 forested granitic catchment (Strengbach, Vosges Mountains, France). *Geochim. Cosmochim. Acta*
462 74, 4612–4628.

463 Liu X.M., Rudnick R.L., McDonough W.F., Cummings M.L. (2013). Influence of chemical weathering on
464 the composition of the continental crust: Insights from Li and Nd isotopes in bauxite profiles
465 developed on Columbia River Basalts. *Geochim. Cosmochim. Acta* 115, 73–91.

466 Liu X.M., Wanner C., Rudnick R.L., McDonough W.F. (2015). Processes controlling delta Li-7 in rivers
467 illuminated by study of streams and groundwaters draining basalts. *Earth Planet. Sci. Lett.* 409,
468 212–224.

469 Machado-Vieira R., Manji H.K., Zarate C.A. (2009). The role of lithium in the treatment of bipolar
470 disorder: convergent evidence for neurotrophic effects as a unifying hypothesis. *Bipolar Disord.*
471 11, 92-109.

472 Marriott C.S., Henderson G.M., Crompton R., Staubwasser M., Shaw S. (2004). Effect of mineralogy,
473 salinity, and temperature on Li/Ca and Li isotope composition of calcium carbonate. *Chem. Geol.*
474 212, 5-15.

475 Meredith K., Moriguti T., Tomascak P., Hollins S., Nakamura E. (2013). The lithium, boron and
476 strontium isotopic systematics of groundwaters from an arid aquifer system: Implications for
477 recharge and weathering processes. *Geochim. Cosmochim. Acta* 112, 20–31.

478 Meybeck M. (1983). Atmospheric inputs and river transport of dissolved substances. *IAHS Publ.* 141,
479 173–192.

480 Millot R., Gaillardet J., Dupré B., Allègre C.J. (2003). Northern latitude chemical weathering rates:
481 clues from the Mackenzie River Basin, Canada. *Geochim. Cosmochim. Acta*, 67, 1305-1329.

482 Millot R., Guerrot C., Vigier N. (2004). Accurate and high-precision measurement of lithium isotopes
483 in two reference materials by MC-ICP-MS. *Geostandards and Geoanalytical Research* 28, 153-159.

484 Millot R., Négrel Ph. (2007). Multi-isotopic tracing ($\delta^7\text{Li}$ - $\delta^{11}\text{B}$, $^{87}\text{Sr}/^{86}\text{Sr}$) and chemical
485 geothermometry: evidence from hydro-geothermal systems in France. *Chem. Geol.* 244, 664-678.

486 Millot R., Négrel Ph., Petelet-Giraud E. (2007). Multi-isotopic (Li, B, Sr, Nd) approach for geothermal
487 reservoir characterization in the Limagne Basin (Massif Central, France). *Appl. Geochem.* 22, 2307-
488 2325.

489 Millot R., Vigier N., Gaillardet J. (2010a). Behaviour of lithium and its isotopes during weathering in
490 the Mackenzie Basin, Canada. *Geochim. Cosmochim. Acta*, 74, 3897-3912.

491 Millot R., Scaillet B., Sanjuan B. (2010b). Lithium isotopes in island arc geothermal systems:
492 Guadeloupe, Martinique (French West Indies) and experimental approach. *Geochim. Cosmochim.*
493 *Acta* 74, 1852-1871.

494 Millot R., Petelet-Giraud E., Guerrot C., Négrel Ph. (2010c). Multi-isotopic composition ($\delta^7\text{Li}$ - $\delta^{11}\text{B}$ - δD -
495 $\delta^{18}\text{O}$) of rainwaters in France: origin and spatio-temporal characterization. *Appl. Geochem.* 25,
496 1510-1524.

497 Millot R., Guerrot C., Innocent C., Négrel Ph., Sanjuan B. (2011). Chemical, multi-isotopic (Li-B-Sr-U-H-
498 O) and thermal characterization of Triassic formation waters from the Paris Basin. *Chem. Geol.*
499 283, 226-241.

500 Millot R., Hegan A., Négrel Ph. (2012). Geothermal waters from the Taupo Volcanic Zone, New
501 Zealand: Li, B and Sr isotopes characterization. *Appl. Geochem.* 27, 677-688.

502 Misra S., Froelich P.N. (2012). Lithium isotope history of Cenozoic seawater: changes in silicate
503 weathering and reverse weathering. *Science* 335, 818–823.

504 Naish C., McCubbin I., Edberg O., Harfoot M. (2008). Outlook of Energy Storage Technologies. Policy
505 Department Economic and Scientific Policy.

506 <http://www.europarl.europa.eu/document/activities/cont/201109/20110906ATT26009/>

507 Négrel Ph., Allègre C.J., Dupré B., Lewin E. (1993). Erosion sources determined from inversion of
508 major, trace element ratios and strontium isotopic ratio in river water: the Congo Basin case.
509 *Earth Planet Sci. Lett.* 120, 59–76.

510 Négrel Ph. (1997). Multi elements chemistry of Loire estuary sediments: Anthropogenic versus
511 natural sources. *Estuar. Coast. Shelf Sci.* 44, 395-411.

512 Négrel Ph., Fouillac C, Brach M. (1997). Occurrence of mineral water springs in the stream channel of
513 the Allier River (Massif Central, France): chemical and Sr isotope constraints. *J. Hydrol.* 203, 143-
514 153.

515 Négrel Ph., Roy S. (1998). Rain chemistry in the Massif Central (France). A strontium isotopic and
516 major elements study. *Appl. Geochem.* 13, 941–952.

517 Négrel Ph., Grosbois C. (1999). Changes in chemical and $^{87}\text{Sr}/^{86}\text{Sr}$ signature distribution patterns of
518 suspended matter and bed sediments in the upper Loire river basin (France). *Chem. Geol.* 156,
519 231-249.

520 Négrel Ph., Grosbois C., Kloppmann W. (2000). The labile fraction of suspended matter in the Loire
521 river (France): multi-element chemistry and isotopic (Rb-Sr and C-O) systematics. *Chem. Geol.*
522 166, 271-285.

523 Négrel Ph., Roy S. (2002). Investigating the sources of the labile fraction in sediments from silicate-
524 drained rocks using trace elements, and strontium and lead isotopes. *Sci. Tot. Env.* 298, 163-181.

525 Négrel Ph., Petelet-Giraud E., Barbier J., Gautier E. (2003). Surface water–groundwater interactions in
526 an alluvial plain: chemical and isotopic systematics. *J. Hydrol.* 277(3-4), 248-267.

527 Négrel Ph., Guerrot C., Millot R. (2007). Chemical and strontium isotope characterization of rainwater
528 in France: influence of sources and hydrogeochemical implications. *Isotope Environ. Health Stud.*
529 43, 179–196.

530 Négrel Ph., Millot R., Brenot A., Bertin C. (2010). Lithium isotopes as tracers of groundwater
531 circulation in a peat land. *Chem. Geol.* 276, 119–127.

532 Négrel Ph., Millot R., Guerrot C., Petelet-Giraud E., Brenot A., Malcuit E. (2012). Heterogeneities and
533 interconnections in groundwaters: Coupled B, Li and stable-isotope variations in a large aquifer
534 system (Eocene Sand aquifer, Southwestern France). *Chem. Geol.* 296, 83–95.

535 Négrel Ph., Petelet-Giraud E. (2012). Isotopic evidence of lead sources in Loire river sediment. *App.*
536 *Geochem.* 27, 2019-2030.

537 Négrel Ph., Millot R. (2019). Behaviour of Li isotopes during regolith development on a granitic
538 bedrock (Massif Central, France): controls on the dissolved load of waters, saprolites, soils and
539 sediments. *Chem. Geol.* 523, 121-132.

540 Négrel Ph., Ladenberger A., Reimann C., Birke M., Demetriades A., Sadeghi M., & the GEMAS Project
541 Team. (2019). GEMAS: Geochemical background and mineral potential of emerging tech-critical
542 elements in Europe revealed from low-sampling density geochemical mapping. *App. Geochem.*
543 111, 104425.

544 Négrel Ph., Millot R., Petelet-Giraud E., Klaver G. (2020). Li and $\delta^7\text{Li}$ as proxies for weathering and
545 anthropogenic activities: application to the Dommel River (Meuse basin). *App. Geochem.* 104674.

546 Penniston-Dorland S., Liu X.M., Rudnick R.L. (2017). Lithium Isotope Geochemistry Reviews in
547 Mineralogy and Geochemistry. 82, 165-217.

548 Petelet-Giraud E., Négrel Ph., Casanova J. (2018). Tracing surface water mixings and groundwater
549 inputs using $\delta^{18}\text{O}$ - $\delta^2\text{H}$ and $^{87}\text{Sr}/^{86}\text{Sr}$ isotope fingerprints at basin scale: the Loire River (France).
550 *App. Geochem.* 97, 279-290.

551 Pistiner J.S., Henderson G.M. (2003). Lithium isotope fractionation during continental weathering
552 processes. *Earth Planet Sci. Lett.* 214, 327-339.

553 Pogge von Strandmann P.A.E., Burton K.W., James R.H., van Calsteren P., Gislason S.R., Mokadem F.
554 (2006). Riverine behaviour of uranium and lithium isotopes in an actively glaciated basaltic
555 terrain. *Earth Planet Sci. Lett.* 251, 134-147.

556 Pogge von Strandmann P.A.E., Porcelli D., James R.H., van Calsteren P., Schaefer B., Cartwright I.,
557 Reynolds B.C., Burton K.W. (2014). Chemical weathering processes in the Great Artesian Basin:
558 Evidence from lithium and silicon isotopes. *Earth Planet. Sci. Lett.* 406, 24–36.

559 Pogge von Strandmann P.A.E., Kasemann S.A., Wimpenny J.B. (2020). Lithium and lithium isotopes in
560 Earth's surface cycles. *Elements*, 16, 253-258.

561 Rivé K., Rad S., Assayag N. (2013). Carbon sources and water-rock interactions in the Allier River,
562 France. *Procedia Earth Planet.* 7, 713-716.

563 Royer T.V. (2016). Human-Dominated Rivers and River Management in the Anthropocene. Book
564 Chapter: Stream Ecosystems in a Changing Environment, 491-524.

565 Rudnick R.L., Tomascak P.B., Njo H.B., Gardner L.R. (2004). Extreme lithium isotopic fractionation
566 during continental weathering revealed in saprolites from South Carolina. *Chemical Geology*, 212:
567 45-57.

568 Teng F.Z., McDonough W.F., Rudnick R.L., Dalpé C., Tomascak P.B., Chappell B.W., Gao S. (2004).
569 Lithium isotopic composition and concentration of the upper continental crust. *Geochim.*
570 *Cosmochim. Acta*, 68, 4167-4178.

571 Teng F.Z., Dauphas N., Watkins J.M. (2017). Non-traditional stable isotopes: Retrospective and
572 Prospective Reviews in Mineralogy and Geochemistry 82, 1-26.

573 Tomascak P.B. (2004). Developments in the understanding and application of lithium isotopes in the
574 earth and planetary sciences. *Reviews in Mineralogy & Geochemistry* 55, 153-195.

575 Tomascak P.B., Magna T, Dohmen R. (2016). *Advances in Lithium Isotope Geochemistry*. ISSN: 2364-
576 5105 Springer.

577 Vanwalleghem T., Gómez J.A., Infante Amate J., González de Molina M., Giráldez J.V. (2017). Impact
578 of historical land use and soil management change on soil erosion and agricultural sustainability
579 during the Anthropocene. *Anthropocene*, 17, 13-29.

580 Viers J. Dupré B., Gaillardet J. (2009). Chemical composition of suspended sediments in World Rivers:
581 New insights from a new database. *Science of the Total Environment*, 407, 853-868.

582 Vigier N., Gíslason S.R., Burton K.W., Millot R., Mokadem F. (2009). The relationship between riverine
583 lithium isotope composition and silicate weathering rates in Iceland. *Earth Planet Sci. Lett.* 287,
584 434-441.

585 Wang Q.L., Chetelat B., Zhao Z.Q., Ding H., Li SL, Wang B.L., Li J., Liu X.L. (2015). Behavior of lithium
586 isotopes in the Changjiang River system: Sources effects and response to weathering and erosion.
587 *Geochim. Cosmochim. Acta* 151, 117–132.

588 Wenshuai L., Liu X.M. (2020). Experimental investigation of lithium isotope fractionation during
589 kaolinite adsorption: Implications for chemical weathering. *Geochimica et Cosmochimica Acta*,
590 284: 156-172.

591 Wiederhold J.G. (2015). Metal stable isotope signatures as tracers in environmental geochemistry.
592 *Environ. Sci. Technol.* 49, 2606–2624.

593 Wimpenny J., James R.H., Burton K.W., Gannoun A., Mokadem F., Gíslason S.R. (2010). Glacial effects
594 on weathering processes: New insights from the elemental and lithium isotopic composition of
595 West Greenland rivers. *Earth Planet Sci. Lett.* 290, 427-437.

596 World Economic Forum (2019). A Vision for a Sustainable Battery Value Chain in 2030. Unlocking the
597 Full Potential to Power Sustainable Development and Climate Change Mitigation.
598 <https://www.weforum.org/reports/a-vision-for-a-sustainable-battery-value-chain-in-2030>
599
600

601 **Figure and Table Captions**

602 **Figure 1:** Map showing the Loire River Basin within France (right). The geological map shows the
603 different sampling points for the Loire River mainstream and the different tributaries.

604 **Figure 2:** Map of the Egoutier watershed. 2a: General location of the sampling points, 2b: Land cover
605 map, 2c: Geological map. Modified from [Desaulty and Millot \(2017\)](#). The locations of the hospital and
606 the industrial area are shown on 2b.

607 **Figure 3:** Li concentrations ($\mu\text{g/L}$, Fig. 3a) and Li isotopic compositions ($\delta^7\text{Li}$, ‰, Fig. 3b) in the Loire
608 mainstream for low- and high-flow stages plotted as a function of distance from the source (km).

609 **Figure 4:** $\delta^7\text{Li}$ (‰) plotted as a function of Na/Li mass ratio for the Loire River mainstream. Na
610 concentrations are from [Desaulty and Millot \(2017\)](#).

611 **Figure 5:** $\delta^7\text{Li}$ rainwater corrected (‰) plotted as a function of Li concentrations after rainwater
612 correction ($\mu\text{g/L}$) for both low- and high-flow water samples. See text for explanation.

613 **Figure 6:** $\delta^7\text{Li}$ (‰) plotted as a function of the Al/Li mass ratio for suspended Loire sediments of the
614 Loire at Montjean. Al data are from [Desaulty and Millot \(2017\)](#). (Determination coefficient $R^2 = 0.60$,
615 Correlation Coefficient $R = 0.78$).

616 **Figure 7:** Li isotopic compositions ($\delta^7\text{Li}$, ‰) in the Loire River sediments at Montjean as a function of
617 river discharge (m^3/s) (Coefficient of determination $R^2 = 0.48$, Correlation coefficient $R = 0.69$).

618 **Figure 8:** Li concentrations ($\mu\text{g/L}$, Fig. 8a) and Li isotopic compositions ($\delta^7\text{Li}$, ‰, Fig. 8b) in Egoutier
619 waters plotted as a function of distance from the source (km).

620

621 **Table 1:**

622 Major elements (Na, Cl), trace (Li) concentrations and Li-isotopic compositions ($\delta^7\text{Li}$, ‰) of Loire
623 waters and its main tributaries, at both high- and low-flow stages. The * means after atmospheric
624 correction (see text for explanations). River discharge data are also reported here.

625 **Table 2:**

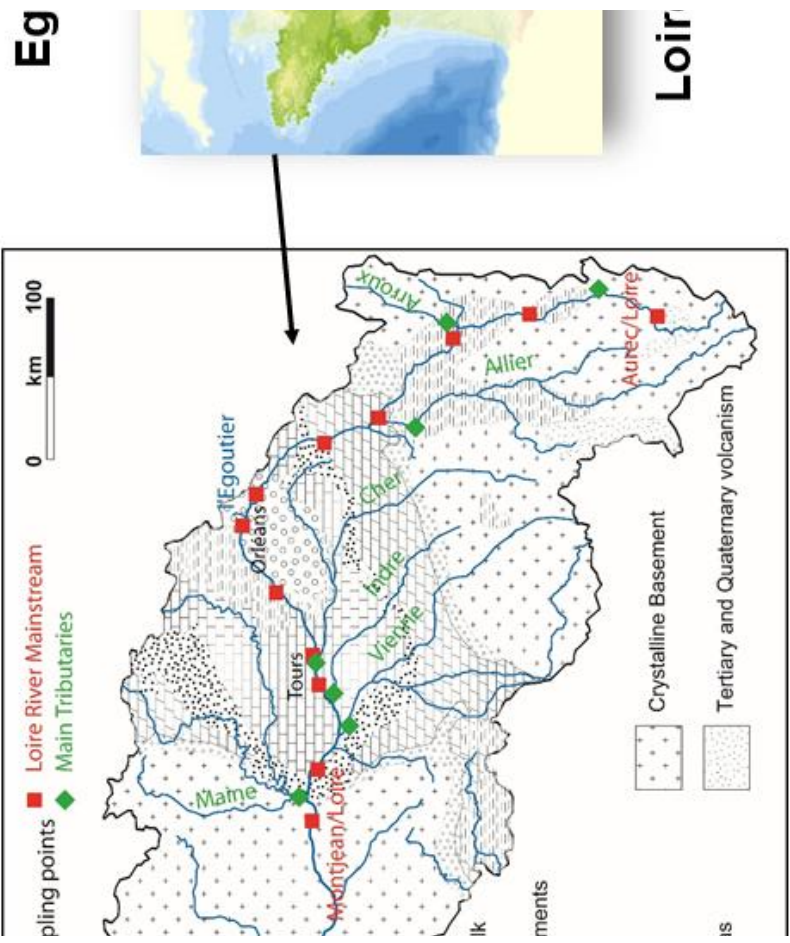
626 Aluminium and Lithium concentrations and Li-isotopic compositions ($\delta^7\text{Li}$, ‰) of suspended river
627 sediments sampled at Montjean/Loire. River discharge data are also reported here.

628 **Table 3:**

629 Li concentrations and Li isotopic compositions ($\delta^7\text{Li}$, ‰) of Egoutier catchment waters.

630

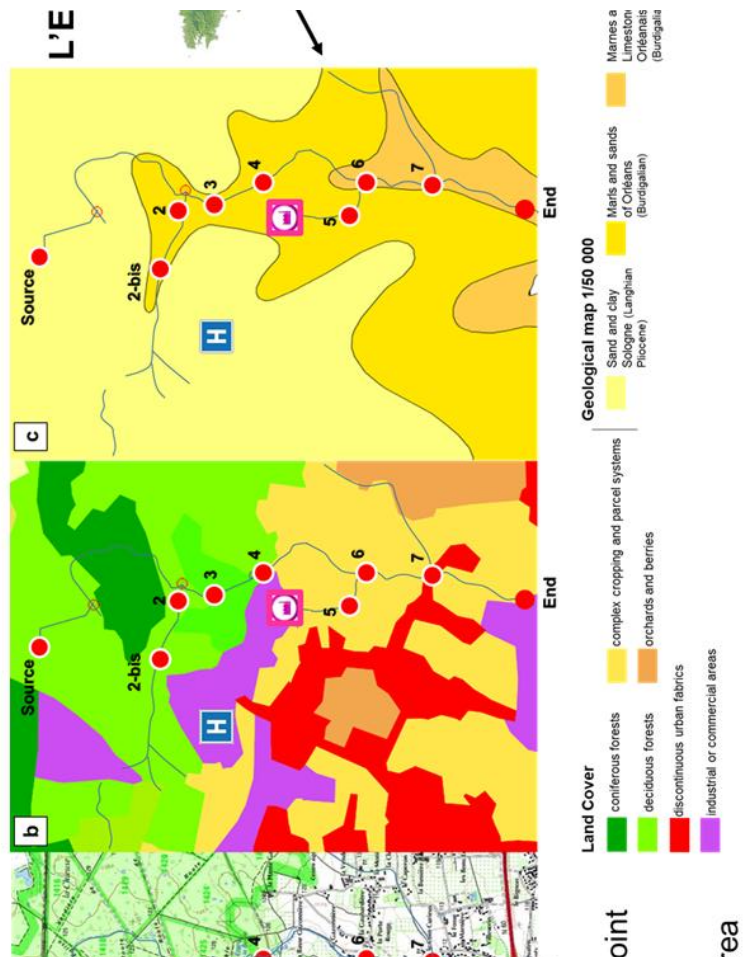
631 Figure 1



632

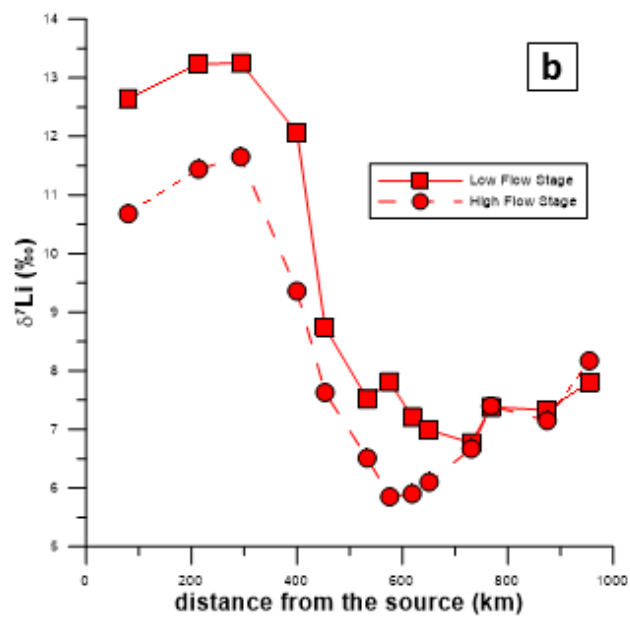
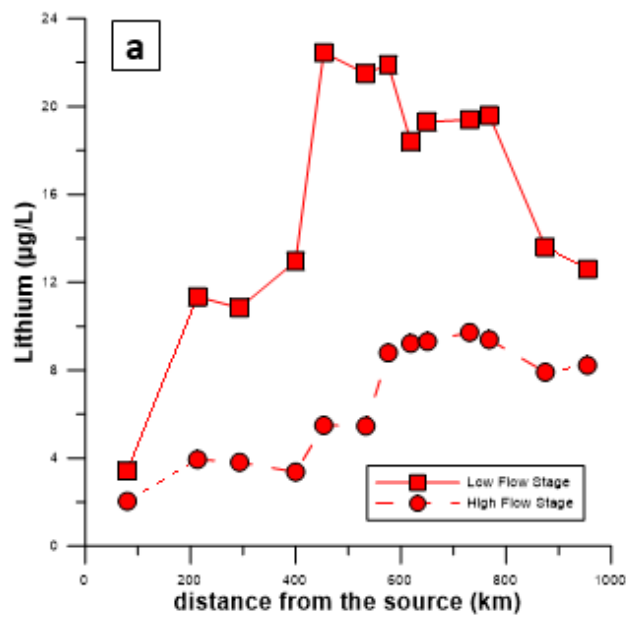
633

634 Figure 2



635

636



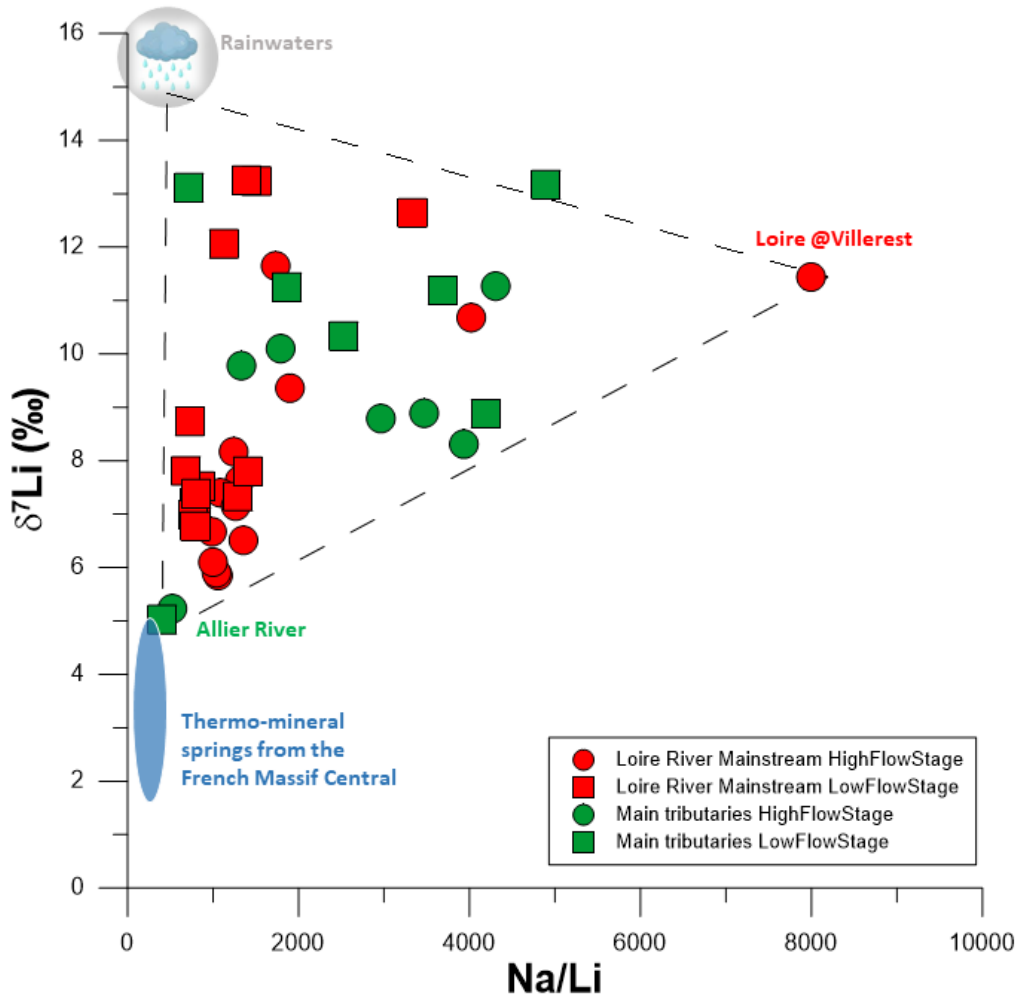
638

639

640

641

642 **Figure 04**

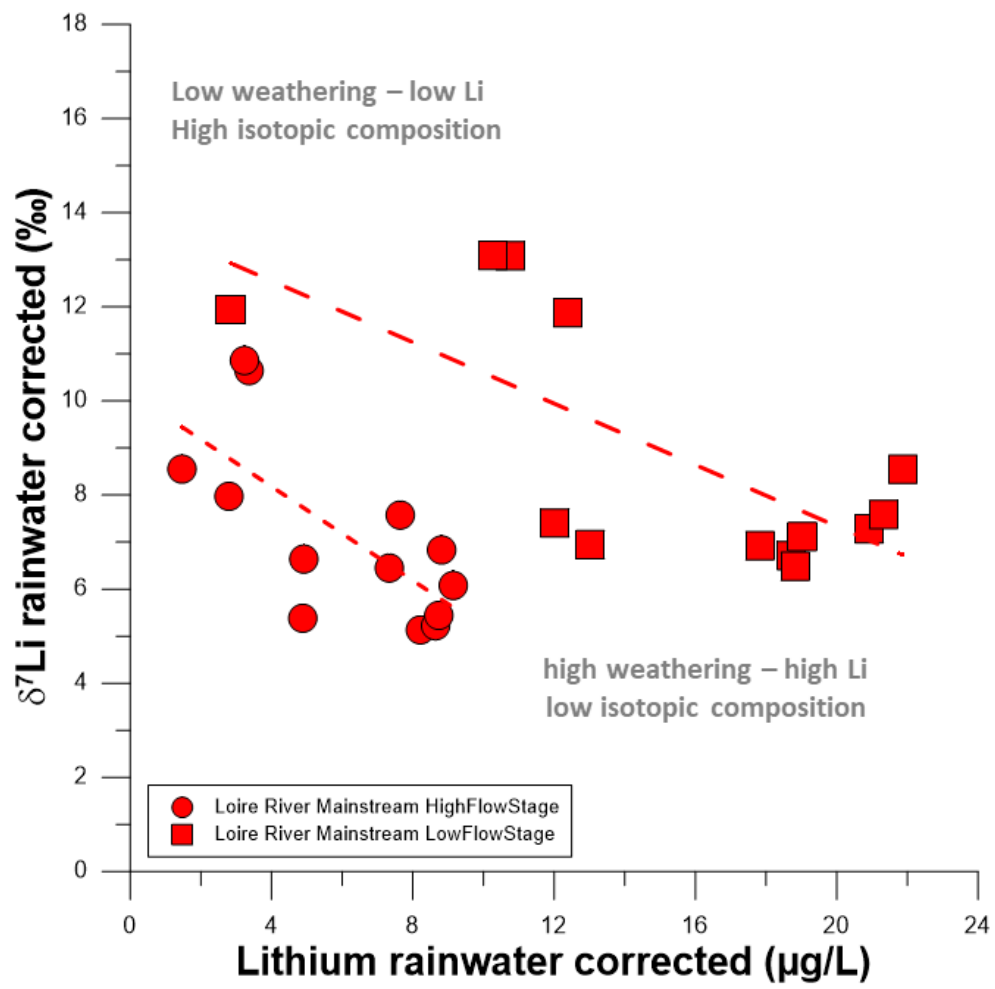


643

644

645

646 Figure 05



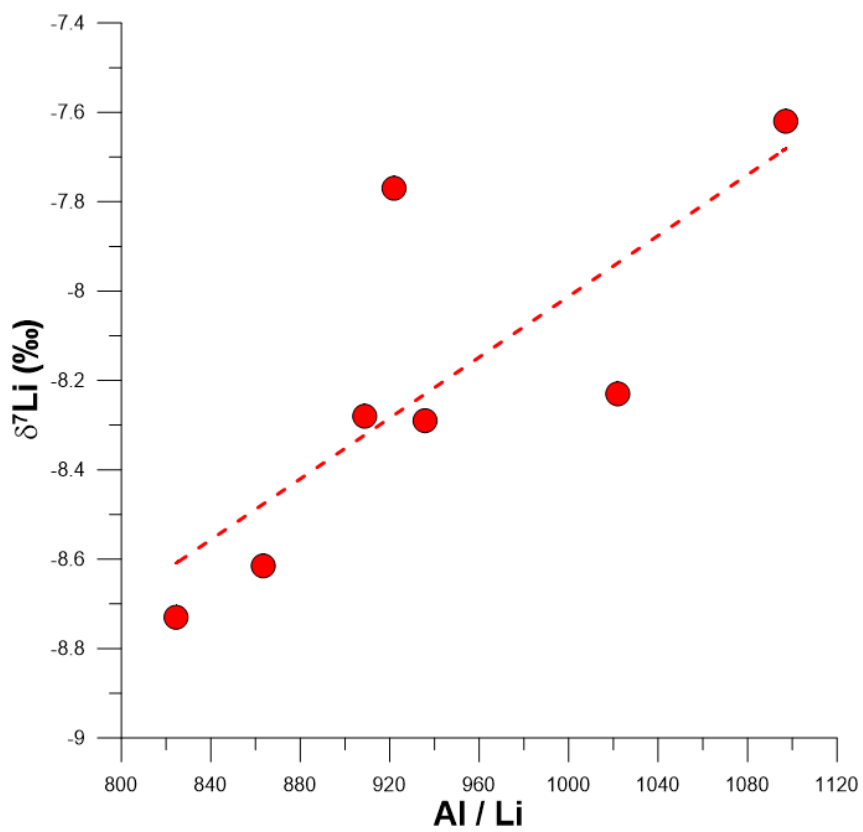
647

648

649

650

651 **Figure 06**



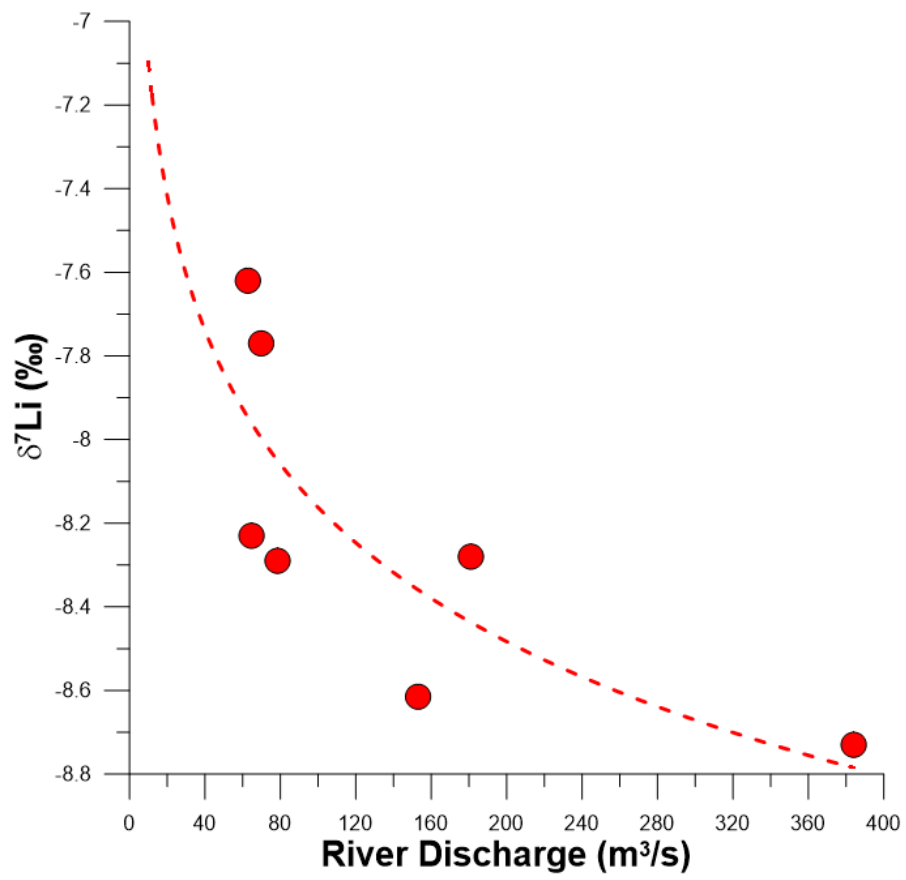
652

653

654

655

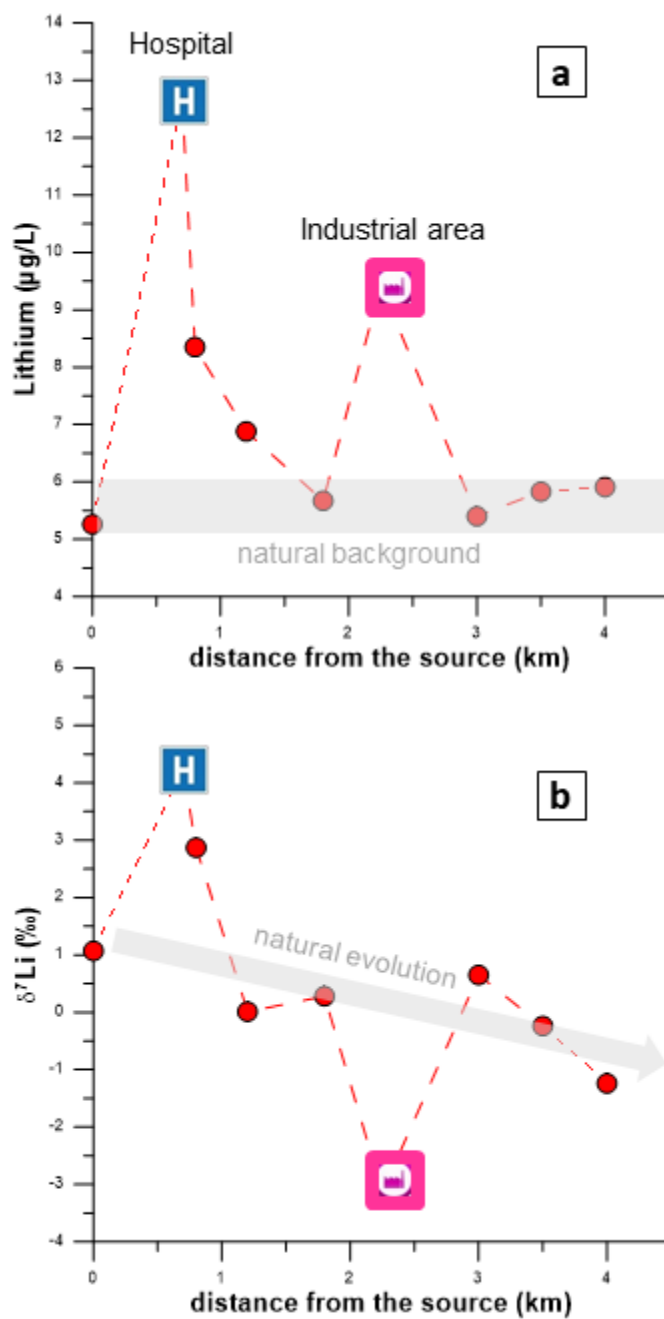
656 **Figure 07**



657

658

659



661

662

663

	W) Cl (low)	Li (low)	Li* (low)	Li* (low)	δ ³⁴ Li (low)	δ ³⁴ Li* (low)	δ ³⁴ Li* (low)	δ ³⁴ Li* (low)	discharge (low)
	mg/L	μg/L	μg/L	μg/L	‰	‰	‰	‰	m ³ /s
1	16.1	3.4	2.8	12.6	11.9	10.7	10.7	10.7	10.7
1	22.7	11.3	10.8	13.2	13.1	41.6	13.1	41.6	41.6
1	21.8	10.8	10.3	13.3	13.1	27.6	13.1	27.6	27.6
1	20.9	13.0	12.4	12.1	11.9	67.0	11.9	67.0	67.0
1	22.2	22.5	21.9	8.7	8.5	89.9	8.5	89.9	89.9
1	23.2	21.5	20.9	7.5	7.3	88.6	7.3	88.6	88.6
1	19.3	21.9	21.3	7.8	7.6	60.4	7.6	60.4	60.4
1	20.2	18.4	17.8	7.2	6.9	60.4	6.9	60.4	60.4
1	21.4	19.3	18.7	7.0	6.7	78.7	6.7	78.7	78.7
1	21.1	19.4	18.8	6.8	6.5	78.7	6.5	78.7	78.7
1	21.9	19.6	19.0	7.4	7.1	77.1	7.1	77.1	77.1
1	22.9	13.6	13.0	7.3	6.9	127.0	6.9	127.0	127.0
1	25.7	12.6	12.0	7.8	7.4	144.0	7.4	144.0	144.0
1	24.4	5.7	5.1	10.3	9.7	9.7	9.7	9.7	9.7
1	30.3	4.8	4.2	11.2	10.5	3.3	10.5	3.3	3.3
1	22.5	4.3	3.7	13.2	12.7	31.4	12.7	31.4	31.4
1	38.4	5.1	4.5	8.9	8.0	-	8.0	-	-
1	73.3	29.9	29.3	11.3	11.2	1.7	11.2	1.7	1.7
1	20.7	14.3	13.7	13.1	13.0	7.7	13.0	7.7	7.7
1	25.1	46.5	45.9	5.0	4.9	37.1	4.9	37.1	37.1

667 **Table 2**

River	Sampling location	Sampling date	Al $\mu\text{g/g}$	Li $\mu\text{g/g}$	$\delta^7\text{Li}$ ‰	discharge m^3/s
Loire	Montjean/Loire	July 2012	45779	56	-8.7	384
Loire	Montjean/Loire	August 2012	46525	51	-8.3	181
Loire	Montjean/Loire	September 2012	50735	59	-8.6	153
Loire	Montjean/Loire	April 2013	75021	68	-7.6	62.75
Loire	Montjean/Loire	May 2013	74611	73	-8.2	64.69
Loire	Montjean/Loire	June 2013	67308	73	-7.8	69.78
Loire	Montjean/Loire	July 2013	38580	41	-8.3	78.47

668

669

670 **Table 3**

671

River	Sampling location	Li	$\delta^7\text{Li}$
		$\mu\text{g/L}$	‰
Egoutier	Source	5.3	1.1
Egoutier	point 2	8.4	2.9
Egoutier	point 2 bis	12.7	4.2
Egoutier	point 3	6.9	0.0
Egoutier	point 4	5.7	0.3
Egoutier	point 5	9.4	-3.1
Egoutier	point 6	5.4	0.7
Egoutier	point 7	5.8	-0.2
Egoutier	end	5.9	-1.2

672